Harla Journals

Harla Journal of Applied Science and Materials

Journal home page: https://journals.ddu.edu.et/index.php/HJASM

Harla journal of Applied Science and Materials

Photoionization Model for Non-Uniform Slow Novae Shells

Belay Sitotaw Goshu[1]

[1]*Department of Physics, College of Natural and Computational Sciences, Dire Dawa University, Dire Dawa, Ethiopia*
Email:belaysitotaw@gmail.com

Abstract

This work aimed to model the properties of a photoionization model and a heterogeneous slow nova shell. I used the "hazy" photoionization algorithm to simulate the flow of the line. Throughout the period, I ran the model with the most abundant elements (H, He, C, N, O, and Ne) having fixed and increasing abundance values. This model can constrain some of the nova region's physical properties, including density, temperature, and ionization structure. The primary driver of temperature variations in the nova envelope, Hii, in novae shells, is chemical heterogeneity. The C, N, O, and Ne frequencies were -1.824, -1.523, -1.398, and -3.000. The low temperature it produces, 840 K, is somewhat warmer than the temperature of an electron. The ionization structure of the electron temperature increases to 0.04 pc from the inner shell and then gradually decreases to 0.08 pc. O^{+3} can also be ionized if the oxygen ionization in the internal boundary area between Hii and He ii is sharp. Forbidden lines are those ions that fall outside of this range. The most common are [O II] and [O III]. The majority of the line fluxes seen in the spectra may be plausibly explained by the model when comparing the observed and predicted line intensities.

Keywords: Abundances; Non-uniform; Novae; photoionization; shells; temperature

1. Introduction

Quasi-binary systems are associated with nova explosions when the secondary star fills the Roche lobe and transfers gas to the disk through accretion to a white dwarf (WD) Geertz, (1988). It is a runaway thermonuclear event on the WD that is increasing in mass. This hydrogen-rich gas accrues on the surface of the WD until its temperature and density reach a point where thermonuclear reactions can begin according to Martin et al. (2000). Once combustion of the unstable hydrogen shell begins, the shell grows significantly and the WD reaches its optical maximum and becomes very bright Hachisu & Kato (2015). The expanding gas has a more metal-rich chemical composition than solar gas, and the heated white dwarf below photo ionized Martin et al. (2000). Unless the cohort star is a wide binary star, the nova explosion causes the WD's shell to expand so much that it swallows up the heavily donating companion star.

**Corresponding author: Belay Sitotew; email: belaysitotaw@gmail.com; Cell phone: +251923694899*

Received: Feburary 2023; Received in revised form: May 2023; Accepted: June 2023

Thermonuclear runaway of degraded material accumulated on the surface of WD, which is an interacting binary star system, is the cause of the eruption. Livius et al. (1990); Scott, (2000).

In classical nova ejections, mass enrichment of heavy elements of to several tens of percent is observed. This increase in WD is thought to begin when accumulated hydrogen diffuses from the WD into the quiescent core (Prialnik, 1986; Kata & Hochisu, 2015). The mass of the WD decreases with each nova burst as the surface of the WD core is eroded and blown away by the nova wind. During an eruption, 10^{-7} to 10^{-3} M of material is lost from the system. The released material is visible for 50 to 100 years. Scott (1900).

As the star orbits within it, thermal energy is produced by the frictional reaction between the companion star and the nova's shell. These frictional processes were thought to be the main cause of reducing envelope ejection and nova lifetimes by more than tenfold in the 1980s. Sources cited in Kato & Hachisu (2011): Donald et al. (1985); Livio et al. (1990); Shankar et al. (1991). This concept was originally developed to understand the long period of nuclear burn (about 1000 years) and the short period of observed classical novae (about 1 year). Nevertheless, in the shell phase of a nova, the accumulation of drag energy for mass ejection is ineffective because the shell mass is too small to generate enough drag energy to eject the shell Donald et al. (1985); Livio et al. (1990); Shankar et al. (1991) cited in Kato & Hachisu (2011).

White dwarfs with nova explosions fall into two categories: carbon-oxygen (CO) and oxygen-neon (ONe). The first one is indicative of the last state of a star with a mass smaller than 10 M. according to Jose & Hernanza (2006), which goes through two evolutionary stages before producing a carbon- and oxygen-rich object (CO) that is sustained by electron pressure: center hydrogen burning and central helium burning. An extra step of non-degenerate carbon ignition is experienced by more massive progenitors, resulting in the production of an oxygen- and neon-rich core (ONe) with traces of sodium and magnesium. According to Jose and Hernanza (2006) and Saizar

et al. (1996), the cut-off mass that somewhat separates the two white dwarf subclasses is approximately 1.1.

The physical explanation for chemical abundances and their ejection from the binary system is given by thermonuclear runaway, which is linked to the populations of CONe in Nova systems. During this process, the expanding gas reaches velocities of 400–4000 km s^{-1}, leading to the nova outburst's abundances being enriched and its departure from the system (Izzo et al., 2015).

According to Matheson et al. (1993) and Moro-Martin et al. (2000), the three most noticeable emission lines in the second kind of novae are [Ne III] λλ3869/3967, [Nev]λλ3346/3426, and [OIII]λλ4959/5007.

I primarily concentrate on the effects of produced heavy element abundances on thermonuclear runaway processes (TNR) to create the model of inhomogeneous slow novae shells. Hence, there is an enrichment of C, N, O, and Ne in the expelled heavy elements. Since additional heavy elements contribute less than fundamental elements to the electron temperature, ionization structure, and line intensity ratio, I ignore them.

Assuming a nonuniform distribution of hydrogen density, which relies on the radial distance from the central stars, Mitchell & Evans (1984), Rawlings (1988), and Bell et al. (1990) conducted earlier work on the ionization structure and the chemistry of novae. Blackbody radiation field, spherically symmetric Solf (1983), ejecta distribution, and Aller et al. (1979) However, the primary element abundances are myprimary focus in this paper; the other characteristics remain unchanged from the prior one.

As in planetary nebulae, supernova leftovers and nova ejected, and the chemical history of galaxies in Hii in my own and other star systems, abundances of chemical elements in gaseous nebulae provide crucial hints to the late stages of stellar evolution. (1990). However, the chemical abundances of helium, carbon, nitrogen, oxygen, and neon which were originally collected from Asplund et al. (2004) are the main emphasis of this work. However, I increased the chemical abundances of C, N, and O in my work by a thousand-fold scale factor according to the findings of Asplund et al. (2004). To calculate the uncertainty in the reddening effect of emission lines, these

abundances are estimated. According to Schwartz et al. (1997), there can be a change in the ionization emission lines relative to the ionization lines due to changes in heavy metal abundances. It's common knowledge that the gases C, N, and O are more enriched than solar values. This aids in myfurther exploration of the Novae shell's ionization structure.

The fundamental reason for temperature differences in Hii, Nova Shells, and planetary nebulae is thought to be chemical inhomogeneities. Various writers (Torres-Peimbert et al., 1990; Kingdon & Ferland, 1998; Peimbert & Peimbert, 2002) have given models. However, this piece differs from them in the following two ways:

i. In comparison to the element abundances provided by Asplund et al. (2004), I increased the primary elements of C, N, and O by various scale factors,

ii. The filling factor is adjusted to fill the vacuum volumes of ejecta varies with the radius.

This work aims to explore, utilizing inhomogeneous chemical abundances and properties such as the photoionization model of the ionized nova shell, the structure of, temperature, and emission lines emitted in the processes of a sluggish novae shell. I aim to explore if the presence of chemical in homogeneities could offer a solution to the novae dilemma through an analogy with the novae shell.

This paper's structure is set up as follows: My photoionization model, together with the input parameters and fundamental presumptions, is explained in Section 2. In addition, I take into account the fundamental model-building characteristics of nova shell radius, density, blackbody temperature, and luminosity. The ionization, emission, and temperature structure of the novae shell are all covered in Section 3, which is then followed by the fundamental presumptions and computations. Additionally, I talk about the differences in the calculated and experimental intensities of lines [O II], [NII], and [O III] for the Nova She in homogeneities. The last section contains my conclusion.

2. Photoionization Model

Photoionization models in studying nova shells utilizing photoionization models in studying nova shells are crucial for understanding the physical properties of these objects. The models can provide information about the mass distribution, elemental

abundances, density, emission lines, and temperature of the nova shells. I used the radiative transfer code CLOUDY version 17.02 to stimulate the slow novae ejection Ferland et al. (2017), which has previously been utilized successively Schwarz, (2002); Vanladingham et al. (2005); Schwarz et al. (2007).
A user can set an incident radiation field, a gas's composition, and its density structure using Cloud.

The temperature and line strength are then obtained by computing the gas's ionization state. The calculation is done in a spherical shape, and the ionic and thermal equilibrium equations are solved to find the electron temperature, ion and electron densities, and line emissivity at each radius from the center ionizing source. The gas distribution with a set of abundances and the description of the ionizing flux using an effective temperature and luminosity serve as the model's inputs.

2.1. Model parameter

To model photoionization and forecast line fluxes, the following elements are considered: H, He, C, N, O, and Ne relative to Hβ. I consider their chemical abundances relative to hydrogen to determine the line intensities. Except for some ions, the dielectronic recombination coefficient has little bearing at low temperatures in novae shells. Relative to the evolved star Osterbrock (1989), observational data reveal that the novae shells are significantly enriched in C, N, and O and moderately enriched in He. Table 2, which displays the derived abundances in Novae 1984's shell, provides an illustration of this.

The relatively low temperature of approximately 500 K is instantly explained by the significant abundances of C, N, O, and Ne mentioned in Table 1. Based on the observed Balmer continuum and the almost complete absence of forbidden lines in the measured spectrum, Williams et al. (1978); and Williams (1982) concluded. The rate of collisionally stimulated far-infrared line radiation is quite significant at this low temperature, leading to a relatively small equilibrium temperature.

Table 1 displays the enhanced values of the populations of the gases He, C, N, O, and Neon in the solar. He is boosted by a factor of two in comparison to the solar values provided by Asplund et al. (2004), while N is 440 times the solar. With scale factors of

50 and 100 times the solar values, respectively, the C and O are relative to the solar values. In this experiment, the helium/hydrogen abundance ratio is greater than in previous works. There are various explanations for this. The first and most significant one is the TNR reactions, which raise helium abundances and occur inside the white dwarf's core. Large helium abundances are produced by helium with low recombination coefficients.

Table 1. Relative abundances of Nova Her 1934 shells*

Elements	Abundances [(Log (Xi/H))]
He	-0.603
C	-1.824
N	1.523
O	-1.398
Ne	-3.000

The algorithm requires additional input parameters, which include the temperature and luminosity of the source (which is presumed to be a blackbody) and those that describe the shell's properties, such as the radius, filling factor, and hydrogen density to account for the novae shell's inhomogeneity. The novae have a smaller inner radius than an outer radius. Photoionization, radiative and dielectronic recombination, charging exchange mechanisms, and gas heating via photoionization in the novae shell are the physical processes taken into consideration.

The high degree of elemental enrichment in novae ejecta, from carbon to neon, indicates a substantial dredge-up of stuff from the underlying white dwarf core and allows novae to contribute to the interstellar medium's chemical enrichment. Scholarly results verify that grains are generated in the processes by observing the epoch of dust creation in the expanding shells of novae. This permits essential limitations to be imposed on the formation process. However, even in the case of grains being injected from novae into solar nebulae, I primarily overlook the effects of dust creation in favor of concentrating on the chemical abundances of C, N, O, and Ne in this work.

2.2. Basic Assumptions

The structure, electron temperature, and emission line fluxes were modeled using the cloudy C17.02 photoionization algorithm used by Ferland et al. (2013). My primary areas of interest are the emission lines and ionization structures of optically thin novae. It resolves the nebula model's thermal and statistical equilibrium. It includes dielectronic recombination, charge transfer, and significant ionization reactions. The

emitted flux predicted by the output is compared to the line fluxes in the spectra that were measured. The fluxes are expressed about Hβ; the model makes no changes to these parameters.

It is assumed that the gas is in thermal and ionization balance, losing all of its output radiation and photoionization from a central source providing the only energy input. In the most basic case, the source of the spectrum is a blackbody with uniform gas density throughout the shell and an effective temperature of 66 000 K. For the core source, the energy luminosity ranges from 10^{36} to 10^{38} erg s^{-1}.

The photoionized nebulae in the spherically symmetric models are centred around an ionizing radiation-emitting central point source. A geometry like this makes sense for H II areas where the core, ionizing OB stars are surrounded by emission gas. It is assumed that with this geometry, the lines of sight toward the source are identical and perceive the same amount of ionizing radiation. Thus, I extended this assumption to the novae shell with local spherical symmetry, when the outburst and the measured expansion velocity are used to create the shell's inner and outer radius. The minimum and maximum velocities of 500 km/s and 1000 km/s, respectively, determine the inner radius of the shell, and the outburst duration is 260 days. Schwarz & Associates (2007) (500 km s^{-1} for 260 days) is found to be 1.12 x 10^{15} cm It was found that the outer radius differed by 2.25 × 10^{15} cm from that reported by Schwarz et al. (1997). Hence, calculations are performed under the assumption of a gas-filling factor that fluctuates according to the power law and is dependent on the radius from the center.

A filling factor of less than one is also permitted in overcast. The ratio of the filled vacuum volumes in the ejecta is determined by the filling factor. It is also believed that the ejecta has spherical symmetry. Due to the absence of comprehensive details regarding the ejecta's geometry and structure, a filling factor that varies with the power-law exponent is provided by

$$f(r) = f(r_o)\left(\frac{r}{r_o}\right)^{\alpha} \qquad (1)$$

where α = −0.5 is the power law index and $f(r_o)$ s the filling factor's beginning value of 0.5. The coverage factor grows with the hazy line luminosities and is defined as the fraction of 4πsr covered by the model shell, which is 0.5. The parameters for nova

shells identified in photoionization model investigations are typically the filling factor given in Eq. 1 and the density index given in Eq. 2.

Building a model whose density fluctuates with the power law allows one to study the influence of inhomogeneity non the novae shell with a gradient of hydrogen density. As a result, the hydrogen density parameter determines the shell's density, whereas the abundance parameters determine the elemental abundances of hydrogen. Cloudy also permits some filling of the shell. The shell's hydrogen density is determined by

$$n(r) = n(r_o)\left(\frac{r}{r_o}\right)^{\beta} \qquad (2)$$

where β is constant and $n\,(r_o)$ is the density of hydrogen at the inner radius r_o

The total mass ejected which is found in the shell can be determined using Eqs 1 and 2 and is given by

$$M_{shell} = n(r_o)f(r_o)\int_{rinn}^{rout}\left(\frac{r}{r_o}\right)^{\beta+\alpha} dV \qquad (3)$$

The shell's volume is expressed as $dV = 4\pi r^2\, dr$. The slow-speed class of novae is consistent with high expelled masses. Slow novae can absorb more mass before exploding because they are thought to occur on less massive white dwarfs than fast novae. In 1997, Schwarz et al. Low-metallicity accreted material does not capture energy like high-metallicity systems do. This permits additional mass to collect in this system, especially WD and accreted material that is discovered close to the TNR peak rather than during the accretion phase Schwarz (2002) and Starrfield et al. (2000). Because clouded uses more interdependent parameters, it is more challenging to determine whether a given solution is unique simply by looking at the generated fields. Thus, I compute the squared provided to select the optimal fir model.

$$\chi^2 = \sum_{i=1}^{n}\frac{(M_i - O_i)^2}{\sigma_i^2} \qquad (4)$$

where O_i is the measured flux ratio, σ_i is the error from the observed flux ratio, M_i is the predicted ratio of line fluxes to hydrogen line flux, and n is the number of lines detected. Depending on the spectral line flux's strength, I estimate an inaccuracy between 10% and 30%. Das and Mondal (2015) For the emission lines employed in this investigation, I chose line ratios of 25%. Hαλ4102, Hγλ4340, [OIII]$\lambda\lambda$4363, 5007, 4959, HeIλ4471, Niλ5679, [NII]5755, He λ5876, [OI]λ6300, 6363, Heiλ6678, and Hα+[NII] λ6563 are the lines that matter. The explanation for the satisfactory $\chi 2$ fit of

a large abundance enhancement model was the combination of big errors and fewer lines. The investigation was unable to reproduce the earlier findings to determine how the parameters fit with the observed emission lines since none of the parameters offered a model that best fit the observed emission lines.

3. Results and Discussion

This study's main goal was to use inhomogeneous chemical abundances and properties such as the photoionization model of the ionized nova shell to explore the temperature, emission lines, and elemental ionization structure of a sluggish novae shell. The shells' moderate enrichment in He and significant enrichment in C, N, and O abundances can be explained by the chemical abundances of the elements shown in Table 1. The exceptionally low temperature of 840 K, which is marginally higher than the temperature of electrons as established by Osterbrock (1989) from the measurement of the Balmer continuum, is produced by the huge abundances of C, N, O, and Ne shown in Table 1.

The low electron temperature is caused by prohibited lines. Figure 1 illustrates how the lines are strong in the early stages of nova shells, but as they expand, the forbidden lines get weaker and electron temperature begins to climb outward before falling to a low temperature. Because of the high rate of collisionally excited far-infrared line radiation at this low temperature, the measured result may not match the equilibrium. The electron temperature's ionization structure rises from the inner shell to 0.04 pc and then steadily decreases to 0.08 pc.

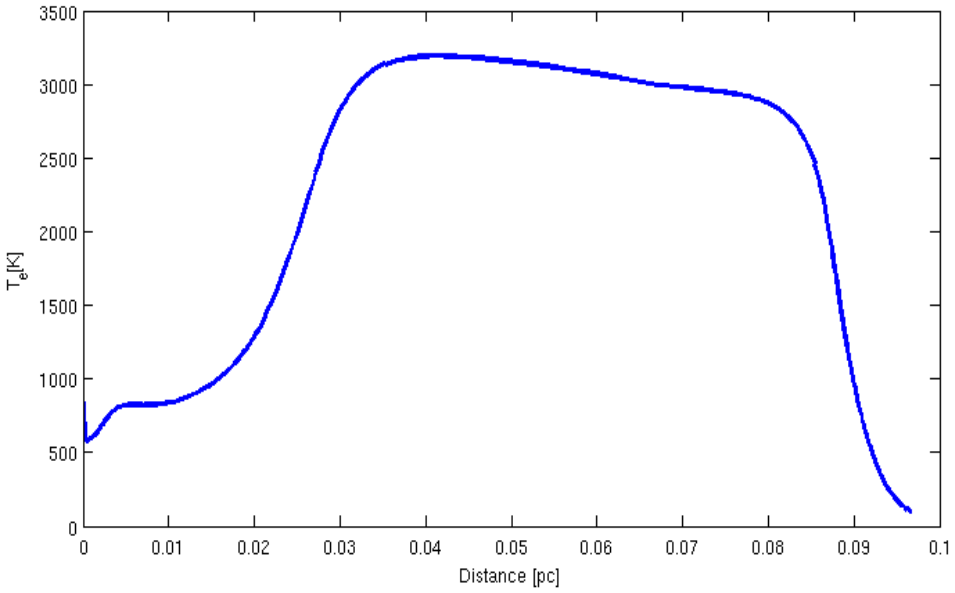

Figure 1. The ionization structure for inhomogeneous nova shell electron temperature

Figure 2 depicts the oxygen ionization structure. He II is a sharp region in the inner boundary zone of Hii, and it can ionize O^{+3}. The other ions, known as forbidden lines [O II] and [O III], are prominent outside of this area. As seen in Figure 2, they have a significant effect in lowering the electron temperature. In this simulation, I observe that the primary source of excitation [O II] λ3727 rather than the Hii area, as depicted in Figure 2, is the photoionization of O^0 by a photon with energy hv > 16.9 eV, leaving O^+ in the excited states term. On the other hand, there is reduced excitation of [O II] λλ5007, 4959. This can be attributed to the fact that [O III] recombination at a quicker rate than [O I] does. Additionally, some lines significantly contribute to cooling.

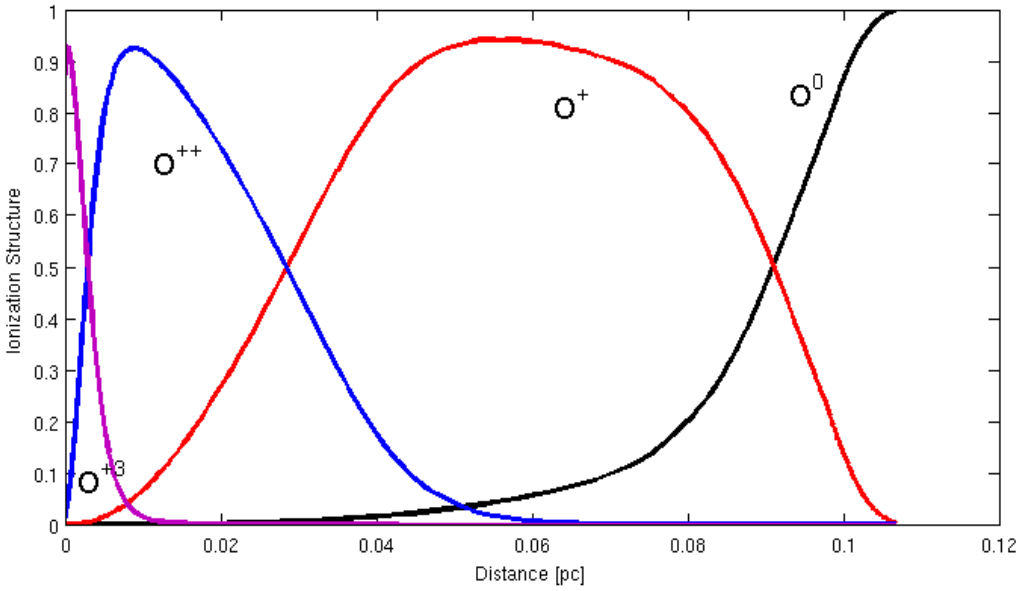

Figure 2. The ionization structure for inhomogeneous nova shell oxygen abundances

The primary cooling lines in nova shells are the result of line radiation from the following line structures: [O III], [N II], and [N III], as well as collisional excitation. Figure 3 illustrates the nitrogen ionization structure at various excitations.

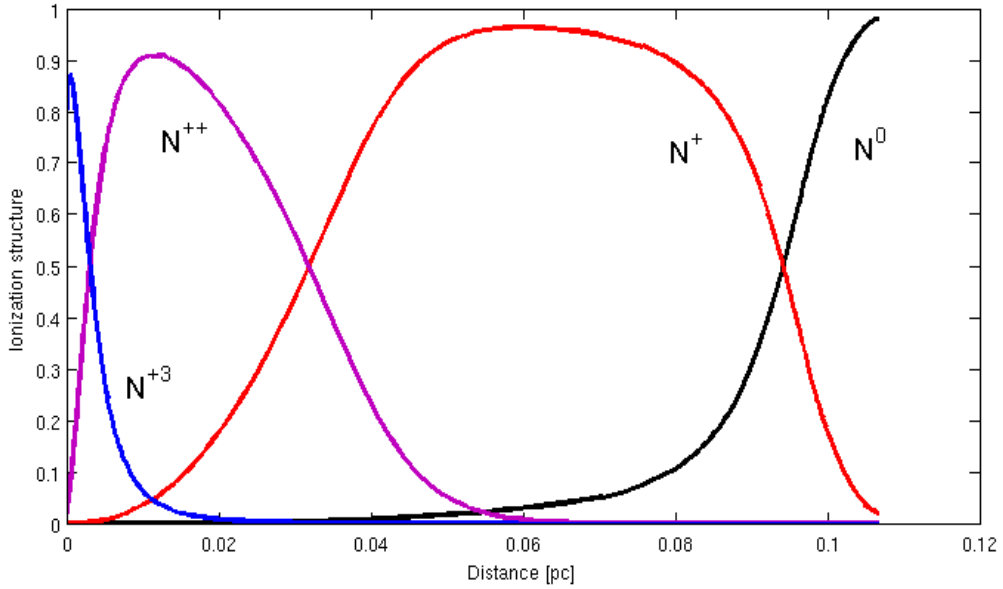

Figure 3. The ionization structure for inhomogeneous nova shell oxygen abundances

The predicted strengths emission flux lines in this model are [O III] λλ52μ, 88μ are 3.42 and 0.623 respectively. The other lines [N II] λ122μ is 2.43 and [N III] λ57μ is 3.06. They are relatively larger than the other forbidden lines shown in Table 2. The expected intensities of emission flux lines linked to particular spectral lines released

by ionized gases inside the nebula were explained by the photoionization hypothesis of a nova shell. Spectral lines emitted by doubly ionized oxygen atoms (O^{2+}) are indicated by the notation "[O III]". The wavelengths of the emitted spectral lines are denoted by λλ52μ and λλ88μ, respectively, and are measured in μm. These emission lines are expected to have intensities of 3.42 and 0.623, respectively. This indicates that the emission from doubly ionized oxygen at 52 μm is dominating over the emission at 88 μm, suggesting that the λ52μ line is substantially stronger than the λ88μ line.

Similarly, spectral lines emitted by singly and doubly ionized nitrogen atoms are indicated by [N II] and [N III]. The wavelengths of the released spectral lines are λ122μ and λ57μ, respectively, measuring 122 and 57 μm. These emission lines are expected to have intensities of 2.43 and 3.06, respectively. This suggests that the emission from nitrogen that has been doubly ionized is stronger at 57 μm than the emission from nitrogen that has been singly ionized at 122 μm.

To sum up, the outcome displays the proportional intensities of emission lines originating from nitrogen and ionized oxygen inside the nova shell. These expected intensities provide information about the physical conditions, ionization state, and composition of the gases within the nebula, as well as the mechanisms driving their emission.

Table 2. The ratio of emission lines relative to Hβ

Line	λ[Å]	Observed	Model	$chi - squared$
Hδ	4102	0.24	0.26	0.006
Hα	6563	4.91	4.05	11.83
Hγ	4340	0.38	0.46	0.11
[O III]	4363	0.3 0.	0.16	0.33
[O III]	5007	0.30	0.16	0.33
[O III]	4959	0.44	0.37	0.08
Hei	4471	0.007	0.07	0.064
Hβ	4861	1.00	1.00	0.00
Nii	5679	0.12	0.154	0.018
[Nii]	5755	1.54	1.12	2.82
Hei	5876	0.29	0.223	0.072
[Oi]	6300	0.11	0.008	0.17
[Oi]	6363	0.05	0.003	0.04
Hei	6678	0.06	0.065	0.0003

A few banned lines, [N II] λ6548 and [O II] λ3727, are found; in Nova Shell, they are likely to arise primarily in the vicinity of the surrounding HII regions. Table 2 displays

most of the lines found in the nova shells. A comparison is made between the calculated and observed line intensity ratios, which both correlate to $\chi 2$. Each line conveys unique information, so it's critical to correctly account for all observational restrictions when fitting the total of the deviations of line intensities to the observed value. There is a discrepancy between the photoionization models' projected values and the measured values of each line flux about Hβ, which correspond to the observed fluxes 15.87 is the total fitting of the line intensity. Furthermore, in all three lines, the [O III]/Hβ intensity ratio was lower than the measured value. The nova shell's inhomogeneity whose mass fluctuates exponentially with distance was the cause of this variation.

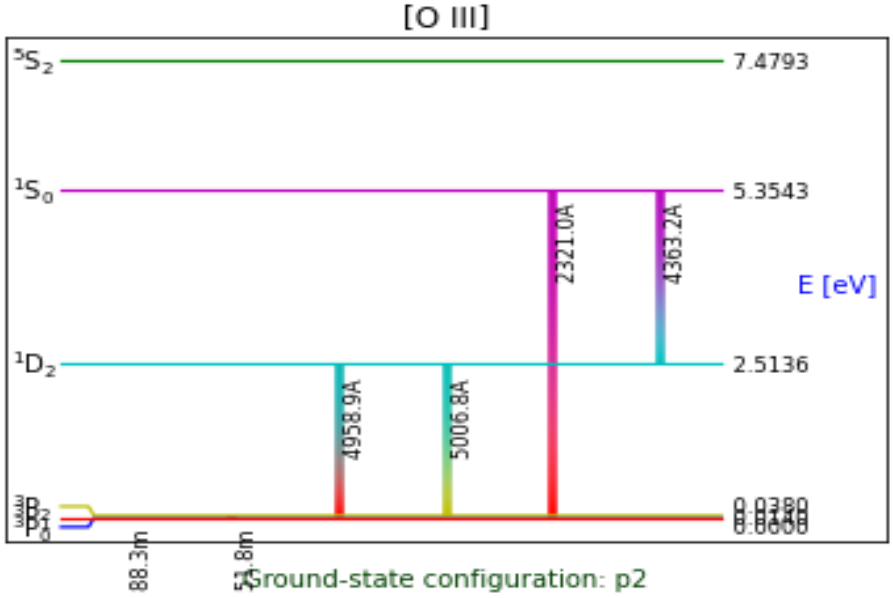

Figure 4. The transition of oxygen lines from the ground state to higher excited states.

The transition figure in Figure 4 illustrates how oxygen line transitions in spectroscopy can be seen from the ground state to higher excited states. The illustration of oxygen atom energy levels and their transitions sheds light on the emission or absorption of electromagnetic radiation, or light, at particular wavelengths. The lowest energy level that an oxygen atom's electrons can reach is known as the ground state. The ground state, also known as the beginning state (E_0), is usually shown at the bottom of the diagram in a transition figure.

When an oxygen atom is in an excited state, its electrons have taken up energy and relocated to higher orbitals, resulting in an energy level above that of the ground state.

The transition figure shows several excited states identified with their respective energy levels (E_1, E_2, E_3, etc.) grouped above the ground state. When oxygen atoms are excited, they can occupy intermediate energy levels momentarily before going back to their ground state.

The results shown in Figure 4 revealed the emission lines of oxygen from the ground state to the excited states. It shows that the transmission lines from ^3P-^1D of [O III]λ5007Å was 2.514 eV, [O III] λ4363Å for ^1D-^1S was 5.354 eV, and for [O III] λ4959Å was 0.013 eV.

4. Conclusions

Using the photoionization code for a model of the inhomogeneous nova shell, I have demonstrated that different inferences about the nature of the nova shell are reached depending on the ionization structure, electron temperature, and ratio of emission lines. The photoionization estimates show discrepancies due to significant variations in elemental chemical abundances and hydrogen density. A thorough photoionization analysis that takes into consideration all the factors influencing the line intensities and the observation apertures is necessary to gain a deeper understanding. Using the photoionization code Cloudy, which can generate the lines, I carried out this study and compared the observed ones. Assuming a volume filling factor of 0.5, which decays exponentially by power factor -0.5, I were able to create a nearly adequate model. The mass of the nova in the shell also changes with the power law with the factor of Hβ.

The work "Photoionization Model for Non-Uniform Slow Novae Shells" makes a substantial contribution to my knowledge of computational astrophysics, interstellar medium parameters, and star development. By interpreting observational data, advancing theoretical models of novae evolution, and constraining star characteristics, it helps astronomers better understand the larger cosmic framework in which novae occurrences occur. Furthermore, the advancement of numerical simulation methods and computational astrophysics is facilitated by the creation and improvement of photoionization models for novae shells. By include intricate physical processes like temperature balancing, ionization equilibrium, and radiation transport, these models

offer a thorough framework for researching the dynamics and evolution of novae systems.

5. Acknowledgments

I would like to express my gratitude to everyone I have had the pleasure of working with on this and other related initiatives. I appreciate the physics department staff for their relentless effort to finish this paper.

6. Conflict of interest

There is no conflict of interest

7. References

Aller L.H., Keyes C.D., & Czyzak S.J, Model nebulae and determination of the chemical composition of the Magellanic Clouds, 1979, Proac. Natal. Acad. Sct. USA.,76, 1525

Aller L.H., The Chemical Composition of gaseous nebulae, 1990, PASP.,102, 1097

A Asplund M., Grevesse N., Sauval A.J., Allende Prieto C., Kiselman D., 2004, The Chemical Composition of the Sun, A&A, 417, 751 Bell H., Gail H.P., Gass H., & Sedlmayr E., 1990, A&A, 238, 283

Das R., & Mondal A., Abundance analysis of the recurrent nova RS Ophiuchi (2006 outburst), 2015, arxiv. 1503.00074v1 [astro-ph. SR]

Ferland G.J., et al. 2017, Hazy: Introduction to cloudy c17.02

Gehrz R.D., 1988, The infrared temporal development of classical novae, ARAA, 26, 377

Izzo L., Valle M. D., Mason E., Matteucci F., Romano D., Pasquini L., Vanzi L., Jordan A., Fernandez J.M., Bluhum P., Brahm R., Espinoza N., and Williams R., Early optical spectra of nova V1369 Cen show the presence of Lithium, 2015, APJ, 808, L14

Jose J., & Hernanza M., 2006, Is drag luminosity effective in recurrent novae? Eur. Phys. J, A 27, 107 Kato M., & Hachisu I, 1991a, ApJ, 373, 620

Kato M., & Hachisu I, 1991b, ApJ, 373, 620

Kato M., & Hachisu I, Recurrent novae as progenitors of Type Ia supernovae, 2012, Bull. Astr. Soc. India, 40, 393–417

Kato M., & Hachisu I, 2015, Acta Polythecnica CTU, 2, 2015

Kingdon J. B., & Ferland G.J., 1998, ApJ, 506, 323

Livio M., Shankar A., Burkert A., Truran J.W., 1990, The Common Envelope Phase in the Outbursts of Classical Novae, ApJ, 356, 250

MacDonald J., Fujimoto M.Y., & Truran J.W., 1985, ApJ, 294, 263

Matheson T., Filippenko A.V., Ho L.C., 1993, ApJ, 418, L29

Mitchell R.M., Evans A., 1984, MNRAS, 209, 945

Moro-Martin A., Garnavich P.M., & Noriega-Crespo A., 2000, arxiv: astro-ph/0012241v1

Osterbrock D.E., 1989, Astrophysics of Gaseous Nebulae and Active Galactic Nuclei, California University of Science book, 2nd edit.

Peimbert M., 2002, in Ionized Gaseous Nebulae, RevMexAACS, 12, 275

Peimbert M., & Peimbert A., 2002, RevMexAASC, in press Prialnik D.: 1986, ApJ 310, 222

Rawlings J.M., 1988, MNRAS, 232, 507

Saizar P., Pachoulakis I., Shore S.N., Starrfield S., Williams R.E., Rothschild E., & Sonneborn G., 1996, MNRAS, 279, 280

Schwarz G.J., Starrfield S., Shore S.N., Hauschildt P.H., 1997, MNRAS, 290, 75

Schwarz G.J., 2002, ApJ, 577, 940

Schwarz G.J., Woodward C.F., Bode M.F., Evans A., Eyres S.P., Geballe T.R., Gehrz R.D., Greenhouse M.A., Helton L.A., Liller W., Lyke J.E., Lynch D.K., O'Brien T.J., Rudy R.J., Russell R.W., Shore S.N., Starrfield S.G., Teimim T., Truran J.W., Venturini C.C., Wagner R.M., Williams R.E., & Zamanov R., 2007, arxiv:0705.0701v1 astro-ph

Schwarz G.J., Shore S.N., Starrfield S., & Vanladingham K.M, 2007, ApJ, 657, 453

Scott A.D., 2000, MNRAS, 313, 775

Shankar A., Livito M., & Truran J. W., 1991, ApJ, 373, 623

Solf J., 1983, ApJ, 273, 647

Sparks W.M., Kutter G.S., Starrfield S., Truran J.W., 1990, in Cassatela A., Viotti R. eds, Proc, IAU, Colloq. 122, Physics of Classical Novae. Springer-Verlag, Berlin, p, 361

Starrfield S., Schwarz G.J., Truran J.W., & Sparks W.M., 2000, in AIP Con.Proc. 522, Cosmic Explosions, ed. S.S. Holt & Zhang W. W. (New York: AIP), 379

Torres-Peimbert S., Peimbert M., & Pe˜na M., 1990, A&A, 233, 540 Vanladingham K.M., Schwarz G.J., Shore S.N., Starrfield S., & Wagner R.M., 2005, ApJ, 624, 914

Williams R.E., 1982 Astrophys. J., 261, 170

Williams R.E., Woolf N.J., Hege E.K., Moore R.L., & Kopriva D.A., 1978. Astrophys. J., 224, 171